

Large-Scale Assessment of Drought Variability Based on NCEP/NCAR and ERA-40 Re-Analyses

ISABELLA BORDI¹, KLAUS FRAEDRICH², MARCELLO PETITTA¹
and ALFONSO SUTERA¹

¹*Department of Physics, University of Rome “La Sapienza”, P.le Aldo Moro 2 00185 Rome, Italy;*

²*Meteorologisches Institut, Universität Hamburg, D-20146 Hamburg, Germany*

(Received: 28 July 2004; in final form: 28 November 2005)

Abstract. The impacts of different spatial resolutions and different data assimilation schemes of the available re-analysis data sets (NCEP/NCAR and ERA-40) on the assessment of drought variability are analysed. Particular attention has been devoted to the analysis of the possible existence of a linear trend in the climatic signal. The long-term aspects of drought over the globe during the last forty years have been evaluated by computing the Standardized Precipitation Index (SPI) on 24-month time scale. The SPI, in fact, seems to be a useful tool for monitoring dry and wet periods on multiple time scales and comparing climatic conditions of areas governed by different hydrological regimes. To unveil possible discrepancies between the analyses carried out with the two data sets, we studied the leading space-time variability of drought by applying the principal component analysis (PCA) to the SPI time series. Results suggest that on the global scale, the two re-analyses agree in their first principal component score, but not in the associated loading: both re-analyses capture a linear trend, though the areas where this feature should be most likely observed are not uniquely identified by the two data sets. Moreover, while the ERA-40 unveils the presence of a weak net “global” trend towards wet conditions, the NCEP/NCAR re-analysis suggests that the areas in the world characterised by positive/negative trends balance to zero. At large regional scale, a good agreement of the results with those obtained from the observations are found for the United States, while for the European sector the two re-analyses show remarkable differences both in the first loading and in representing the timing of the wet and dry periods. Also for these areas a linear trend, superposed on other short-term fluctuations, is detectable in the first principal component of the SPI field.

Key words: drought assessment, re-analysis data, large-scale variability, standardized precipitation index, principal component analysis

1. Introduction

An assessment of drought conditions in a particular area and its spatial-temporal variability plays an important role in the development of practices for water resources management and for the planning of measures devoted to the mitigation of the negative impacts of future occurrences. For these purposes, several studies have been carried out to develop objective methods for the evaluation of water supply deficit, the estimation of the duration time of precipitation shortages or the return time of dry events (see Keyantash and Dracup, 2002, for a review).

However, the reliability of these analyses strongly depends on the quality of the primary data. In particular, in assessing dry or wet periods, it is highly desirable to have at hand a data set that: (i) is easy to access, (ii) uniformly covers the globe, (iii) has a time-duration sufficiently long to be trustworthy in a statistical sense and (iv) is optimal in the sense of capturing consistently dry and wet events. Most of the available records may match one or more of these requirements, but not (especially the first) all of them. Thus, in meteorological studies it has become a popular practise to disregard raw observations in favour of “analysed data”, i.e. a set of observations which have been processed through several quality checks, including the ones of their consistency with atmospheric models of a great complexity. In meteorology, the analysed fields are the result of complex interactions between available observations and model results. The final products of this procedure are uniformly gridded fields on a global scale of wind, temperature, specific humidity and mass that are released for further applications. In the latest decade or so, two of such re-analyses became easily available: one produced by the National Centers for Environmental Prediction/National Center for Atmospheric Research (NCEP/NCAR) and the other one by the European Centre for Medium-Range Weather Forecasts (ECMWF), the ERA-40.

Let us remark that precipitation, the main variable for drought assessment, is not a primary variable of the re-analysis product, i.e. the observed precipitation is not assimilated in the model, but it is evaluated by the physical model that has assimilated other data. Thus it is fair to define the re-analysed precipitation as a forecast product.

In principle, these data satisfy the criteria above described and, therefore, they may be used to assess dry or wet periods over the globe for approximately the last fifty years. At the best of our knowledge, apart from few exceptions (Bordi *et al.*, 2001), the optimality, for the assessment of dry/wet periods, of these re-analyses has not been reported. Moreover, a comprehensive check of such re-analyses and their reliability against observations is not yet available, especially when the purpose is the evaluation of the long-term aspects of climatic features, such as dry and wet periods. In particular, an intercomparison between the performances of the two re-analyses in capturing the trend unveiled in some regions using observations (such as Sicily and China, Bonaccorso *et al.*, 2003; Bordi *et al.*, 2004) is virtually absent. Given the great deal of relevance in understanding the trend shown by dry and wet spell analysis over the globe and the high potential in doing so by means of re-analysis, the present paper is devoted to such an achievement, by sorting the positive outcomes and signalling the negative ones.

At this aim, we decide to use, as an indicator of dry and wet periods, the Standardized Precipitation Index (SPI) as defined by McKee (1993) and widely applied in drought monitoring centres (see for example the National Drought Mitigation Center web site <http://drought.unl.edu>) or in some case studies (Hayes *et al.*, 1999; Loukas and Vassiliades, 2004; Tsakiris and Vangelis, 2004; Lloyd-Hughes and Saunders, 2002 or Bordi *et al.*, 2001, 2002, 2004 for its use in combination with

a re-analysis product). This index, based only on precipitation, is, in fact, a useful tool for capturing most of the climate variability associated with water shortage or surplus in different areas. Moreover, we compute also the SPI over grid points over the ocean. This may appear an unusual and exotic practice, but we argue that most of driest or wettest events occur over the oceans. As we will see later on, the assessment of the climate variability in these locations may unveil remote connections among, apparently local, climate features. Therefore, the meaning of the SPI may go beyond its usual understanding by acquiring the significance of climate variable.

Since the number of grid points available to us is far behind our capability of assessing climate fluctuations at each location, we decide to extract the main variability by using a principal component analysis, excluding however, any further rotation to preserve the global nature of the climatic signal.

The paper is organised as follows. In section 2 data and methods for the analysis are presented, while in Section 3 the main results for the globe, the United States and the Euro-Mediterranean area are shown. In the final section some conclusions and discussions are put forward.

2. Data and Methods of Analysis

2.1. DATA

The analysis is based on monthly precipitation time series, from which drought is monitored. The two data sets used, the NCEP/NCAR and the ECMWF 40-yr re-analysis (ERA-40), have different spatial resolutions and different assimilation schemes have been applied in their re-analysis procedures. The ERA-40 precipitation data are available at $2.5^\circ \times 2.5^\circ$ regular latitude/longitude grid, while those from the NCEP/NCAR have $1.9^\circ \times 1.9^\circ$ horizontal resolution. The ECMWF data are provided every six hours and it is possible to download total precipitation or its different components (say convective and stratiform precipitation), while daily or monthly precipitation rates are available for the NCEP/NCAR data set. The NCEP/NCAR reanalysis, which is available back to 1948, comprises different data sources such as observations from land stations and ships, upper air rawinsondes, satellite and numerical weather forecasts, which are assimilated in an AGCM (Atmospheric Global Circulation Model) and re-analysed by means of a “frozen” state of an AGCM (for more information see Kalnay *et al.*, 1996). The ECMWF 40-year re-analysis project (ERA-40, Simmons and Gibson, 2000, Uppala, 2002) has been recently finalised and the data are available for climatic studies. This analysis of the state of the atmosphere, which covers the period from September 1957 to August 2002, complements the hitherto available NCEP/NCAR and ERA-15 re-analyses. The ERA-40 project applies a modern Variational Data Assimilation technique (used in daily operational numerical forecasting at ECMWF) to the past conventional and satellite observations.

Because the two data sets cover different periods, we choose the common one ranging from January 1958 to December 2001. We carry out the analysis for the

globe and the Euro-Mediterranean region (the area selected is 27.5° – 70° N, 12.5° – 62.5° E). We also show the analysis for the United States derived from the CPC (Climate Prediction Center, U.S.) unified precipitation data set (Higgins *et al.*, 2000). This Unified Raingauge Dataset (URD) has been established from multiple sources of U.S. raingauge data. Tests to eliminate duplicates and overlapping stations, standard deviation and buddy checks were applied; subsequent gridding into $0.25^{\circ} \times 0.25^{\circ}$ (20° – 60° N, 140° – 60° W) was accomplished by using a Cressman (1959) scheme. The data set covers the period from January 1958 to December 1998 and we use this period for the analysis over the United States.

2.2. STANDARDIZED PRECIPITATION INDEX (SPI)

Drought conditions of the areas under study have been assessed by applying the SPI. The index permits to monitor both dry and wet periods and requires for its computation only long time series of monthly precipitation. The SPI is computed by fitting a probability density function to the frequency distribution of precipitation summed over a selected time scale (usually 1, 3, 6, 12 and 24 months are used). This is performed separately for each month of the year and each location in space. Each probability density function is then transformed into the standardised normal distribution, which readily allows comparison between distinct locations and analytical computation of exceedance probabilities. Thus, the SPI is a Z-score or the number of standard deviations (above or below) that an event deviates from the normalised mean of the month considered. Values of the standardised normal variable are grouped into classes that identify the severity level of a drought or a wet event (McKee *et al.*, 1993; Bordi and Sutera, 2001).

Because the index can be computed for multiple time scales by considering the cumulated precipitation over a selected period, different effects of wetness/dryness can be specified: short time scales affect growing seasons, long time scales characterise hydrologic balances with a net water gain/loss. The time scale of 24 months is usually considered a suitable time scale for the investigation of the long-term aspects of dryness and wetness (see Keyantash and Dracup, 2002), thus we decide to focus our analysis on this time scale.

2.3. PRINCIPAL COMPONENT ANALYSIS (PCA)

The leading time and spatial variability of drought has been investigated applying the Principal Component Analysis (PCA) to the SPI on 24-month time scale (SPI-24). The PCA is a classical statistical method widely used in data analysis, for identifying patterns, and compression, reducing the number of dimensions. The method consists of the following steps (see for example Rencher, 1998 or Peixoto and Oort, 1992). From a sample of vectors x_1, \dots, x_M of n components ($i = 1, \dots, n$), we can calculate the sample mean (μ_x) and the sample covariance matrix (C_x). Thus, from a symmetric matrix such as the covariance one, we can calculate an orthogonal basis by finding its eigenvalues (λ_i) and eigenvectors (e_i),

which are the solutions of the characteristic equation:

$$|C_x - \lambda I| = 0,$$

where I is the identity matrix having the same order than C_x and $|\cdot|$ denotes the determinant of the matrix. By ordering the eigenvectors in the order of descending eigenvalues (largest first), one can create an ordered orthogonal basis with the first eigenvector having direction of largest variance of the data. In this way, it is possible to find directions in which the data set has the most significant amounts of variance. Let A be a matrix consisting of eigenvectors of the covariance matrix as the row vectors, by projecting the original data vector on the orthogonal base we get the so called “principal components (PC) scores” as:

$$y = A(x - \mu_x).$$

On the other hand, the original data can be reconstructed using the property of an orthogonal matrix $A^{-1} = A^T$, where the up-script T denotes the transpose:

$$x = A^T y + \mu_x.$$

In the present work, the input data for the PCA are the time series of the SPI-24 at each grid point. Moreover, the SPI time series, by definition, have zero mean, thus in our case $\mu_x = 0$. In guiding a proper interpretation of the results shown in the next section, we remark that the spatial patterns (eigenvectors), properly normalised (divided by their Euclidean norm and multiplied by the square root of the corresponding eigenvalues), are called “loadings”; they represent the correlation between the original data (in our case, the SPI-24 time series at single grid points) and the corresponding principal component time series.

To reduce the degrees of freedom, we may select only few spatial patterns to represent the statistical properties of the original field. However, there is no general rule to decide how many eigenvectors should be retained, though few methods have been proposed (Rencher, 1998). One of these criteria is based on the percentage of variance accounted for, i.e. it is recommended to achieve a relatively high percentage, say 70–90%. For our purpose we focus the attention on the main pattern of variability that explains the most percentage of variance of the SPI-24 field, leaving the latter problem open for other investigations.

3. Global Scale and Regional Analyses

Let us consider, as shown in Figure 1a and b, the first loadings obtained by decomposing the total variance of the SPI-24 by means of a PCA for both ERA-40 and NCEP/NCAR data. They explain respectively 28.2% and 18.2% of the total variance (see Table A1 in the Appendix also for the statistics described later on in

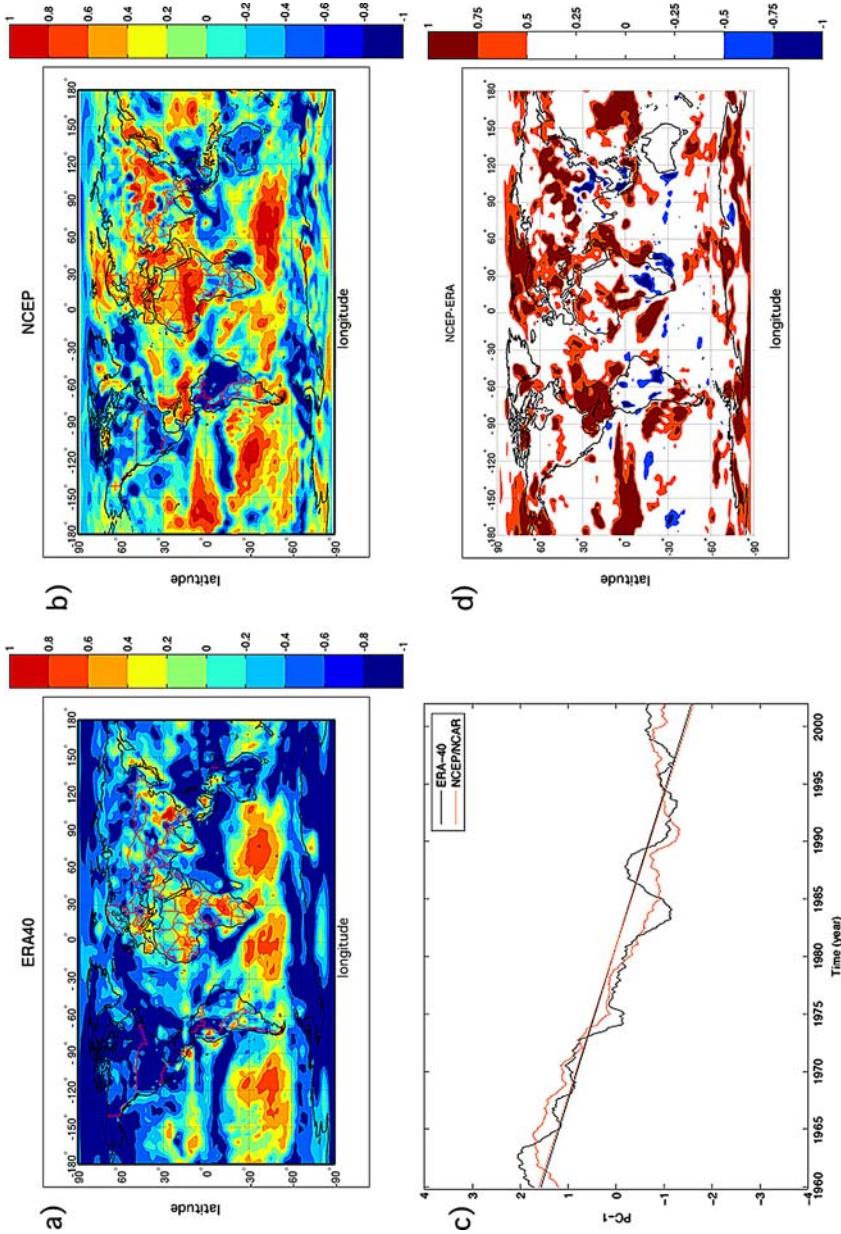


Figure 1. (a) First loading pattern of the SPI-24 for the globe obtained using the ERA-40 data set, contour interval is 0.2; (b) as in a) but for NCEP/NCAR data set; (c) first PC scores for ERA-40 (black line) and NCEP/NCAR (red line), straight lines denote the fitted linear trends; (d) differences between the first loading of NCEP/NCAR and that of ERA-40, absolute values less than 0.5 are denoted by white colour.

the text). The associated principal component scores are shown in Figure 1c. The two signals have a high correlation coefficient (0.96) and denote a long-term linear trend (see the straight lines in the figure) crossing the time axis around the eighties. In the Appendix (see Table A2) values of the angular coefficients and intercepts, with the corresponding error bands at 95% confidence level, are listed together with the Sum Square Error and the R-square statistics. It can be noted that the two re-analyses unveil a common linear trend in the first principal component of the SPI-24 field, which explains more than 80% of the total variation of the signal. The presence of this long-term trend means that, looking Figure 1a and b, the red (blue) areas have been switched from prevalent wet (dry) conditions to prevalent dry (wet) conditions. In particular, the first loading for ERA-40 has positive correlation with the corresponding score greater than 0.5 in about 5.4% of the total grid points and negative correlation less than -0.5 in about 44.9% of points. For NCEP/NCAR the percentage of grid points showing values greater than 0.5 is about 15.0%, while that with values less than -0.5 is about 13.5%. This means that in most of grid points the SPI-24 time series for ERA-40 have a high anti-correlation with the PC score shown in Figure 1c; such behaviour is not confirmed by the NCEP/NCAR data set. On the other hand, the integrals in spherical coordinates of the first loadings provide values of -0.16 for ERA-40 and 0.03 for NCEP/NCAR, denoting the presence of a weak “global” trend towards wet conditions for the ECMWF re-analysis and the absence of a “global” linear trend for the other data set, i.e. the areas in the world characterised by positive/negative trends balance themselves.

Moreover, it must be noted that the features characterising the loadings appear to unveil a relationship among climate fluctuations in seemingly remote areas. Thus, for example, the equatorial Pacific behavior covaries with mid-latitude regions at least for the time scale of the SPI here considered. However, when we inspect the locations where this long-term trend covaries the most, we easily detect striking differences between the two data sets. In illustrating more quantitatively these differences we first interpolate the two loadings on a common grid of $1^\circ \times 1^\circ$ degree and then compute their difference (NCEP minus ERA-40, see Figure 1d). It can be seen that the two loadings have a good agreement (absolute differences less than 0.5) in about 65.3% of the points, with a prevalence of positive differences greater than 0.5 (32.3% of points) with respect to negative (2.4% of points) in the remaining points. Thus, we may conclude that in the last forty years or so, a linear trend in the SPI-24 is detected by the two independent data sets, although the locations where this trend should be observed most likely remain not uniquely identified by the two re-analyses.

To be sure that these differences are not due to the coarse spatial resolution of the ERA-40 precipitation field, we employed the ‘kriging’ technique (Cressie, 1991) to this data set and repeated the analysis (say, we compute the SPI-24 and apply the PCA). The analysis (here not shown) provides results in agreement with those obtained by using the original precipitation data, suggesting that the origin of the detected differences cannot be uniquely attributed to the spatial resolution.

In ascertaining if the source of the above discrepancies are related to the performance of the PCA on a global scale, we investigate the PCA decomposition on large but limited areas where the two global loadings appear close or moderately close, namely the U.S.A. and the European sector. Notice that, roughly speaking, this area reduction is equivalent to a rotation of the first few eigenvectors. For the first area we have also the opportunity to check the two re-analyses against a data set (URD), which is in compliance with the requirements outlined in the introduction and it is easy to get from the web (<http://www.cdc.noaa.gov>).

3.1. CONTINENTAL U.S.A.

Over the continental U.S.A., the first loadings of the SPI-24 for URD, ERA-40 and NCEP/NCAR are shown in Figure 2a–c. They explain, respectively, 22.0%, 64.2% and 38.3% of the total variance. The associated PC scores are displayed in Figure 2d. As for the global case, a long-term trend, embedded on other short-term fluctuations, is recognizable for ERA-40, NCEP/NCAR and URD cases, strongly supporting the assertion about the existence of this feature. Moreover, the first PC scores from ERA-40 and NCEP/NCAR correlate about 0.84, while they correlate with that from URD respectively 0.78 and 0.88. At variance of the global case, the trend statistics, shown in the Appendix, suggests that the parameters of the linear fitting for the re-analyses and observations are different at 95% confidence level and that the fits explain different percentages of the total principal components variations (ERA-40 shows the highest value, about 72.5%). However, although we cannot firmly conclude that the three data sets unveil the same linear trend, we surely may conclude that there is a high degree of similarity and that both re-analyses reasonably comply when compared with observations.

This similarity is reflected also by the first loadings: the absolute differences in the first loadings of NCEP and ERA (again interpolated to the same $1^\circ \times 1^\circ$ grid) are less than 0.5 in about 97.7% of grid points and the main differences (about 2.3%) are concentrated in the south-eastern and northern part of the Continental U.S.A. Furthermore, the two loadings show a good agreement also with the first loading obtained with the observations (URD, see Table A1 for details). On these grounds, one is led to think that each re-analysis may be a good proxy for data.

3.2. EUROPEAN SECTOR

Next, in Figure 3a–c the first loading patterns and scores of the SPI-24 computed for the European area using ERA-40 and NCEP/NCAR precipitation data are shown. They explain, respectively, 22.9% and 21.7% of the total variance. Both PC scores are characterised by a linear trend superimposed to short-term fluctuations, which provide a low degree of co-variability between the two signals. The correlation coefficient of the two PC scores is, in fact, 0.53. The trend statistics suggests that the linear fits explain different percentages of the scores variability (ERA-40 about

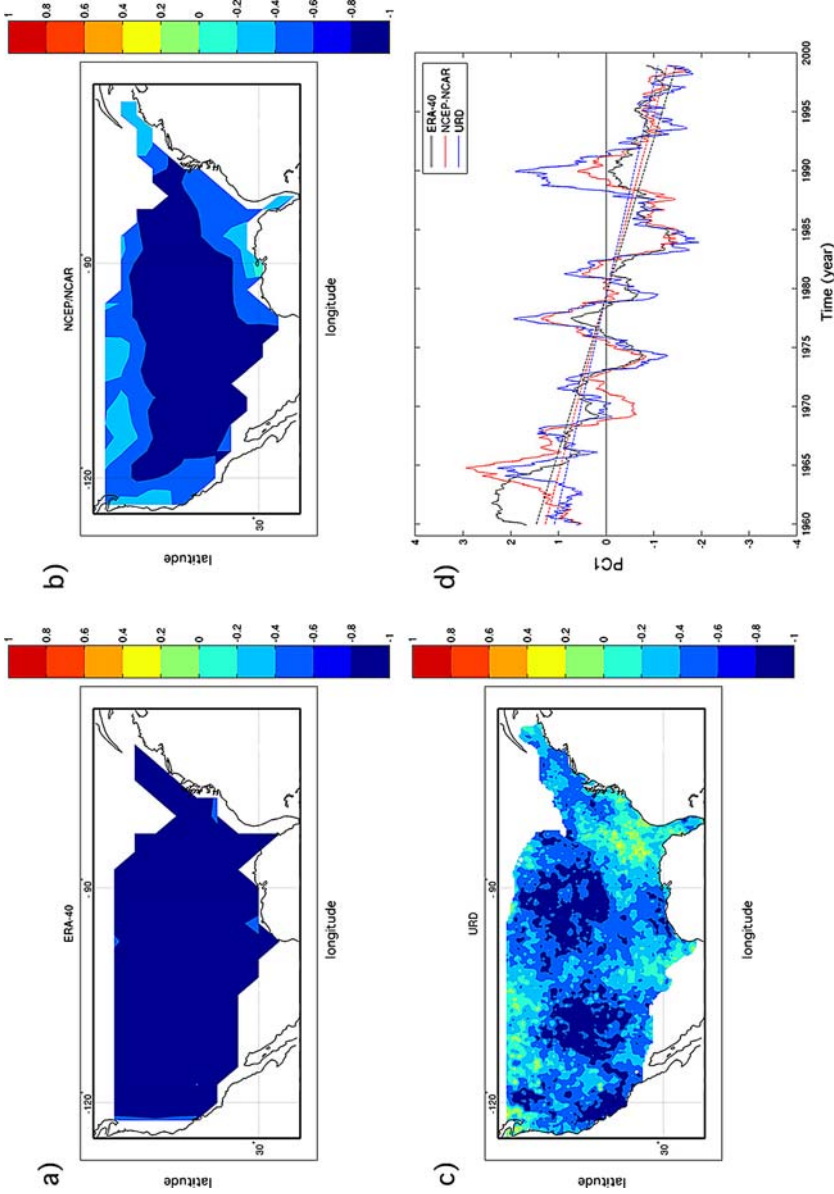


Figure 2. (a) First loading pattern of the SPI-24 for Continental U.S.A. obtained using the ERA-40 data set, contour interval is 0.2; (b) as in (a) but for NCEP/NCAR data set; (c) as in (a) but for URD data set; (d) first PC scores for ERA-40 (black line), NCEP/NCAR (red line) and URD (blue line), straight lines denote the fitted linear trends.

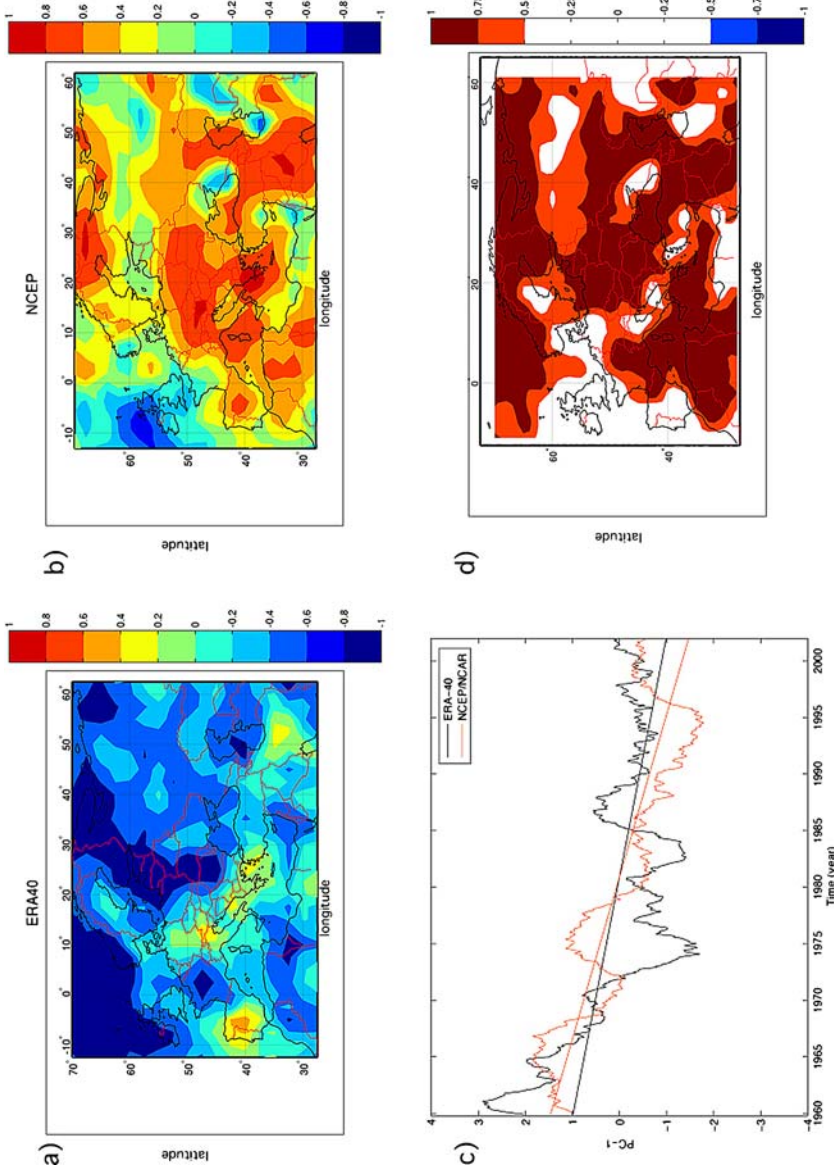


Figure 3. (a) First loading pattern of the SPL-24 for the Euro-Mediterranean sector obtained using the ERA-40 data set, contour interval is 0.2; (b) as in (a) but for NCEP/NCAR data set; (c) first PC scores for ERA-40 (black line) and NCEP/NCAR (red line), straight lines denote the fitted linear trends; (d) differences between the first loading of NCEP/NCAR and that of ERA-40, absolute values less than 0.5 are denoted by white colour.

33% and NCEP about 72%) even if the NCEP/NCAR trend is within the error band of that for ERA-40.

On the other hand, the leading spatial pattern for ERA-40, shows positive correlation between the SPI-24 time series and the corresponding score in the Balkans, Italy, central Europe and Spain, and negative correlations elsewhere. The first loading for NCEP/NCAR, instead, reaches maximum values in North Africa, central Spain, north-eastern Europe, part of Italy, Balkans, Greece and Middle Orient. For ERA-40 the first loading has no grid points with values greater than 0.5, while about 39% of grid points have values less than -0.5 . The NCEP/NCAR loading, instead, has positive values greater than 0.5 in about 37% of points, while values less than -0.5 in only 2% of points. This means that the loading for ERA-40 shows prevalent negative correlations between the SPI-24 time series and the corresponding PC score, with opposite occurrences in the case of NCEP/NCAR.

Although the spatial patterns seem to preserve the main features shown by the global scale analysis, some discrepancies are now more noticeable. From a comparison of the loadings (see Figure 3d) no discernable pattern may be recognised, since the two maps differ virtually everywhere. The two loadings, in fact, have a good agreement (absolute differences less than 0.5) only in about 22% of the points, and in the remaining points the loading differences are strictly positive and greater than 0.5. However, we must point out that the agreement between the two re-analyses is dependent on the area selected as the European sector; better results might be obtained by choosing other areas.

To shed light on these discrepancies we directly compare the index time series, instead of loadings and scores, and proceed as follows. We consider a location over Europe where a remarkable difference between the first loadings have been detected, i.e. where the SPI-24 time series for ERA-40 has a negative correlation with the PC-1 (i.e. the trend), while the index time series for NCEP/NCAR has positive correlation with the corresponding score.

For instance, let consider the ERA-40 grid point at 50.0N-25.0E and the nearest four points in the NCEP/NCAR grid (say 50.53N-24.38E, 50.53N-26.25E, 48.63N-24.38E, 48.63N-26.25E). Next, we compute the SPI-24 time series averaged over the latter points. The time behaviours of these SPI series are shown in Figure 4. The signals have a correlation coefficient of about 0.1, justifying the lack of correlation when the first principal component is considered. It must be noted, however, that, up to the seventies, the two re-analyses show a remarkable different SPI behaviour, while in the remaining part of the record the two series seems to be more alike. Thus, we suspect that the low correlation between the two SPI time series is mainly related to the differences occurring at the beginning of the record, which are crucial in determining the first principal component linear trend. Since in this early decade the data considered had a lower resolution (satellite data were virtually absent), we may suggest that the observed difference may be attributed to the two assimilating models. Thus, a careful analysis of the two models may lead to an understanding of the observed discrepancies.

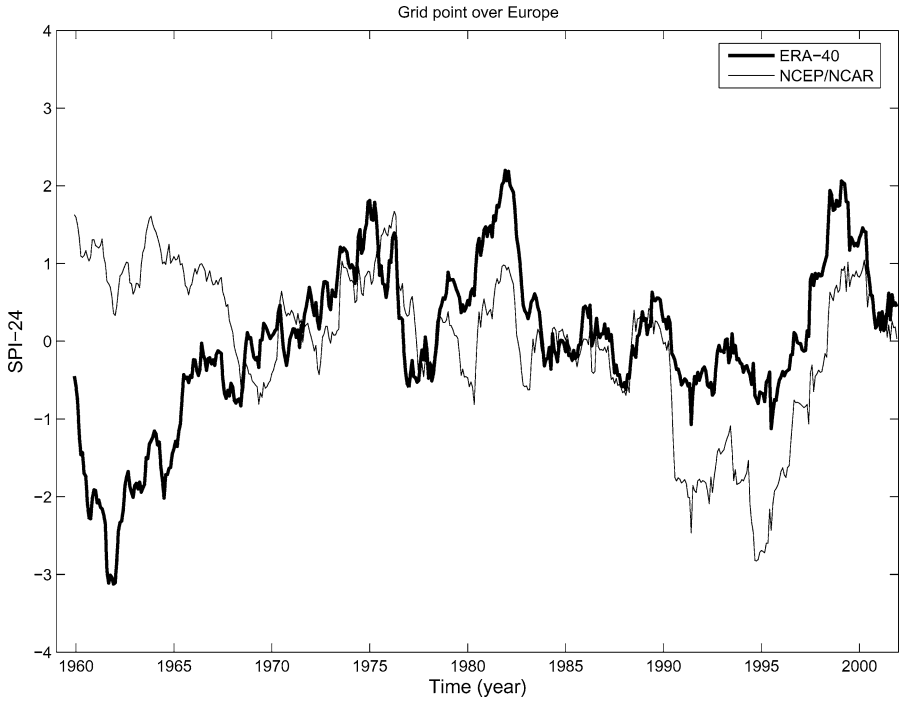


Figure 4. SPI-24 time series at a selected location over Europe (see the text): thick line refers to ERA-40 data set, thin line to NCEP/NCAR.

4. Summary and Conclusions

The aim of the paper was to compare the performances of two re-analyses in capturing the linear trend unveiled in some regions of the world by observations or General Circulation Models which, nowadays, is considered as the most important feature of the climatic signal. The long-term aspects of dry and wet periods over the globe have been evaluated by computing the Standardized Precipitation Index over 24-month time scale. The index computation has been based on the available ERA-40 and NCEP/NCAR re-analysis precipitation data. Then, the leading spatial-temporal variability of dryness and wetness has been assessed by applying the Principal Component Analysis to the SPI time series.

Results suggest that there are noticeable differences between the analyses carried out with ERA-40 and NCEP/NCAR products that cannot be attributed to the different spatial resolutions of the two precipitation fields. On the global scale, the two re-analyses agree in their first principal component score, but not in the associated loading: both re-analyses capture a linear trend, though the areas where this feature should be observed most likely are not uniquely identified by the two data sets. Most importantly, while the ERA-40 unveils the presence of a weak “global”

trend towards wet conditions, the NCEP/NCAR re-analysis suggests that the areas in the world characterised by positive/negative trends balance to zero.

At continental scale, a good agreement of the results with those obtained from the observations are found for the United States, while for the European sector the two re-analyses show remarkable differences both in the first loadings and in representing the timing of the wet and dry periods. Also for these areas a linear trend is detectable in the first principal component of the SPI-24 field, although the sum square errors of the linear fits are higher compared to the global case. Moreover, an analysis carried out in a particular location over Europe suggests that probably some differences between the two re-analyses might be related to remarkable discrepancies occurring in the first part of the precipitation record.

In concluding, results show that both re-analyses capture a trend as a primary feature of the climatic signal, which is present both at global and large regional level, though the spatial location of this climatic behaviour differs greatly between the two re-analysed data sets. The discrepancies unveiled may be related to the different assimilation schemes adopted to produce the re-analysis products; thus, a more stringent comparison with the rain gauge observations would be useful to properly adopt the re-analysis as a tool for drought monitoring purposes. Given that the detected trend may be associated to a climate change, our study suggests that, in the last few decades, there have been some winners and some losers. Unfortunately, the present re-analyses do not allow to uncover who is in one category or in the other.

Acknowledgements

NCEP/NCAR and CPC US Unified Precipitation data have been provided by the NOAA-CIRES Climate Diagnostics Center, Boulder, Colorado, USA, from their Web site at <http://www.cdc.noaa.gov>, while the ERA-40 precipitation data set by the European Centre for Medium-Range Weather Forecasts from their web site <http://www.ecmwf.int>.

Bordi, Petitta and Sutera acknowledge the financial supports provided by the EU Project INTERREG IIIB –MEDOCC-SEDEMED II (code 2003–03–4.4–I–010).

We are grateful to the anonymous reviewers who provided useful comments that improved the presentation of the paper.

Appendix

Comparison among the first loadings and PC scores: In the following Table A1 all the information relative to the first loading and score of the SPI-24 for the globe, United States and Europe, obtained using the precipitation data from ERA-40, NCEP/NCAR and URD data sets, are summarised.

Table A1. Information relative to the first loading and score of the SPI-24 for the globe, United States and Europe, obtained using the precipitation data from ERA-40, NCEP/NCAR and URD data sets

GLOBE	Percentage of variance explained by the first loading	
	ERA	28.2%
	NCEP	18.2%
	PC-1:	
	Corr. Coeff. between ERA and NCEP	0.96
	NCEP loading	
	Grid points with values >0.5	15.0%
	Grid points with values <-0.5	13.5%
	ERA loading	
	Grid points with values >0.5	5.4%
	Grid points with values <-0.5	44.9%
	Loading differences (NCEP-ERA)	
	Grid point with absolute differences < 0.5	65.4%
	Grid point with differences >0.5	32.3%
	Grid point with differences <-0.5	2.3%
U.S.A	Percentage of variance explained by the first loading	
	URD	22.0%
	ERA	64.2%
	NCEP	38.3%
	PC-1	
	Corr. Coeff. between ERA and NCEP	0.84
	Corr. Coeff. between URD and ERA	0.78
	Corr. Coeff. between URD and NCEP	0.88
	NCEP loading	
	Grid points with values >0.5%	0.0%
	Grid points with values <-0.5	68%
	ERA loading	
	Grid points with values >0.5	0.0%
	Grid points with values <-0.5	98.5%
	URD loading	
Grid points with values >0.5	0.0%	
Grid points with values <-0.5	39.3%	
Loading differences (NCEP-ERA)		
Grid point with absolute differences < 0.5	9.7%	
Grid point with differences >0.5	2.3%	
Grid point with differences <-0.5	0.0%	
Loading differences (ERA-URD)		
Grid point with absolute differences < 0.5	79.6%	

(Continued on next page)

Table A1. (Continued)

	Grid point with differences >0.5	0.0%
	Grid point with differences <-0.5	20.4%
	Loading differences (NCEP-URD)	
	Grid point with absolute differences < 0.5	94.8%
	Grid point with differences >0.5	0.0%
	Grid point with differences <-0.5	5.2%
Europe	Percentage of variance explained by the first loading	
	ERA	22.9%
	NCEP	21.7%
	PC-1	
	Corr. Coeff. between ERA and NCEP	0.53
	NCEP loading	
	Grid points with values >0.5	37.3%
	Grid points with values <-0.5	2.0%
	ERA loading	
	Grid points with values >0.5	0.0%
	Grid points with values <-0.5	39.1%
	Loading differences (NCEP-ERA)	
	Grid point with absolute differences < 0.5	21.8%
	Grid point with differences >0.5	78.2%
	Grid point with differences <-0.5	0.0%

TREND ANALYSIS

The fitting process requires a model that relates the observed data to the predictor data with one or more coefficients. To obtain the coefficient estimates, the least squares method is commonly used, which minimizes the summed square of residuals (SSE). The residual (r) for the i th data point n is defined as the difference between the observed response value y_i and the fitted response \hat{y}_i ; and is defined as the error associated with the data:

$$r_i = y_i - \hat{y}_i$$

$$SSE = \sum_{i=1}^n r_i^2 = \sum_{i=1}^n (y_i - \hat{y}_i)^2$$

In our case, to unveil the presence of a long-term trend, we use the linear least squares method to fit a linear model to the first principal component time series of the SPI-24. Thus, we have:

$$\hat{y} = PC1 = p_1 t + p_2,$$

with p_1 , p_2 the coefficients of the linear model and t the time.

Table A2. Values of the angular coefficients and the intercepts, with the corresponding error bands at 95% confidence level, of the linear trend detected in the first PC score of the SPI-24 for the three areas considered and for the different precipitation data sets used for the computation of the index. The last two columns of the table refer to the Sum Square Error (SSE) and the R-square statistics.

Area	Data set	$p_1(\text{year}^{-1})$ with 95% confidence bounds	$p_2(\text{dimensionless})$ with 95% confidence bounds	SSE	R-square
Globe	ERA-40	-0.0749 (-0.0779, -0.0719)	148.4 (142.5, 154.3)	85.8	0.8298
	NCEP	-0.0769 (-0.0795, -0.0744)	152.4 (147.3, 157.4)	62.9	0.8751
U.S.A.	ERA-40	-0.0754 (-0.0796, -0.0712)	149.3 (140.9, 157.6)	128.5	0.7254
	NCEP	-0.0658 (-0.0712, -0.0604)	130.2 (119.6, 140.9)	209.5	0.5523
	URD	-0.0559 (-0.0622, -0.0497)	110.7 (98.3, 123.0)	281.4	0.3987
Europe	ERA-40	-0.0471 (-0.0530, -0.0412)	93.3 (81.59, 105.00)	338.7	0.3266
	NCEP	-0.0698 (-0.0736, -0.0660)	138.3 (130.8, 145.8)	140.7	0.7208

In Table A2 we summarize the values of the angular coefficients (p_1) and the intercepts (p_2), with the corresponding error bands at 95% confidence level, of the linear trend detected in the first PC score of the SPI-24 for the three areas considered and for the different precipitation data sets used for the computation of the index. The last two columns of the table refer to the SSE and the R-square statistics. A value of SSE closer to 0 denotes a better fit. The R-square statistic measures how successful the fit is in explaining the variation of the data and is expressed as:

$$R - \text{square} = 1 - \frac{\text{SSE}}{\text{SST}}$$

where the SST is the sum of squares about the mean and is defined as $\text{SST} = \sum_{i=1}^n (y_i - \bar{y})^2$. It must be noted that in our case the PC scores are standardised, thus we have $\bar{y} = 0$. The R-square can take on any value between 0 and 1, with a value closer to 1 indicating a better fit. For example, an R^2 value of 0.8298 means that the fit explains 82.98% of the total variation of the data about its average.

References

- Bonaccorso, B., Bordi, I., Cancelliere, A., Rossi, G., and Sutera, A., 2003, 'Spatial variability of drought: An analysis of the SPI in Sicily', *Water Resour. Manage.* **17**, 273–296.
- Bordi, I. and Sutera, A., 2001, 'Fifty years of precipitation: Some spatially remote teleconnections', *Water Resour. Manage.* **15**, 247–280.
- Bordi, I. and Sutera, A., 2002, 'An analysis of drought in Italy in the last fifty years', *Nuovo Cimento* **25 C**, 185–206.
- Bordi, I., Fraedrich, K., Jiang, J.-M., and Sutera, A., 2004, 'Spatio-temporal variability of dry and wet periods in eastern China', *Theor. Appl. Climatol.* **79**, 81–91.
- Cressie, N. A. C., 1991, *Statistics for Spatial Data*, New York, John Wiley & Sons, 900 pp.
- Cressman, G.P., 1959, 'An operational objective analysis system', *Mon. Wea. Rev.* **87**, 367–374.
- Hayes, M. J., Svodoba, M. D., Wilhite, D. A., and Vanyarkho, O. V., 1999, 'Monitoring the 1996 drought using the standardized precipitation index', *Bull. Amer. Meteor. Soc.* **80**, 429–438.

- Higgins R. W., Shi, W., Yarosh, E., and Joyce, R., 2000, 'Improved US Precipitation Quality Control System and Analysis', NCEP/Climate Prediction Center ATLAS No. 6.
- Kalnay, E. and co-authors, 1996, 'The NCEP-NCAR 40 year reanalysis project', *Bull. Amer. Meteor. Soc.* **77**, 437–471.
- Keyantash, J. and Dracup, J. A., 2002, 'The quantification of drought: An evaluation of drought indices', *Bull. Amer. Meteor. Soc.* **83**, 1167–1180.
- Lloyd-Hughes, B. and Saunders, M. A., 2002, 'A drought climatology for Europe', *International Journal of Climatology* **22**, 1571–1592.
- Loukas, A. and Vasiliades, L., 2004, 'Probabilistic analysis of drought spatiotemporal characteristics in Thessaly region, Greece', *Natural Hazards and Earth System Sciences* **4**, 719–731.
- McKee, T. B., Doesken, N. J., and Kleist, J., 1993, 'The relationship of drought frequency and duration to time scales', Preprints, *8th Conference on Applied Climatology*, 17–22 January, Anaheim, CA, pp. 179–184.
- Peixoto, J. P. and Oort, A. H., 1992, *Physics of Climate*, Springer-Verlag New York, Inc., 520 pp.
- Rencher, A. C., 1998, *Multivariate Statistical Inference and Applications*, John Wiley & Sons, Inc., 559 pp.
- Simmons, A. J. and Gibson, J. K., 2000, The ERA-40 project plan. ERA-40 Project Report Series 1, ECMWF, Reading, U.K., 62 pp.
- Tsakiris, G. and Vangelis, H., 2004, 'Towards a drought watch system based on spatial SPI', *Water Resour. Manage.* **18**, 1–12.
- Uppala, S., 2002, ECMWF Reanalysis 1957–2001, ERA-40 Project Series 3 Workshop on Reanalysis. ECMWF, Shinfield Park, Reading RG2 9AX.